Supplement

for the reply to Reviewer 2's comments

Multidecadal Variability and Predictability of Antarctic Sea Ice in GFDL SPEAR_LO Model

Yushi Morioka[1,2,3], Liping Zhang[2,4], Thomas L. Delworth[2],
Xiaosong Yang[2], Fanrong Zeng[2], Masami Nonaka[1], Swadhin K. Behera[1]

1: Application Laboratory, VAiG, JAMSTEC, Yokohama, Kanagawa, Japan
2: Geophysical Fluid Dynamics Laboratory, NOAA, Princeton, New Jersey, USA
3: Atmospheric and Oceanic Sciences Program, Princeton University, Princeton, New Jersey, USA
4: University Corporation for Atmospheric Research, Boulder, Colorado, USA

Apr 17, 2023

Submitted to The Cryosphere

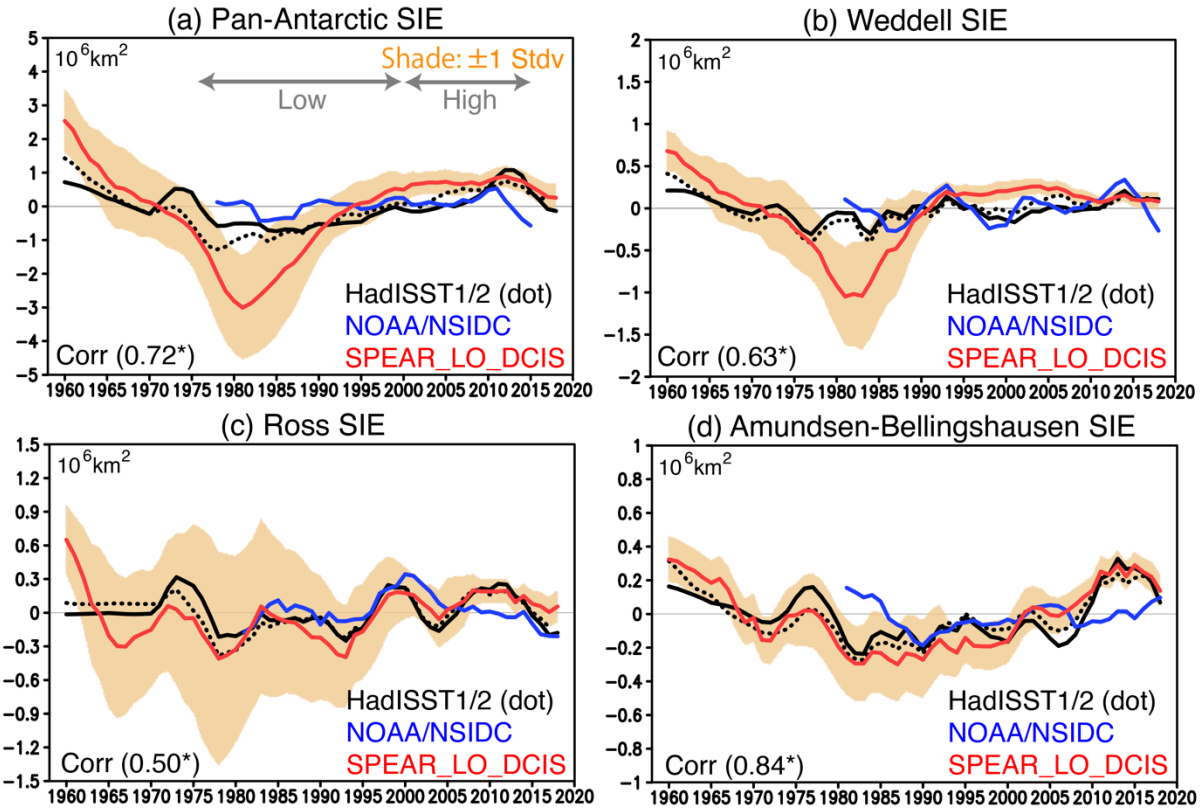

Figure 2 (a) Time series of 5-yr running mean sea ice extent (SIE in 10^6 km^2) anomalies in the pan-Antarctic region during 1958-2020. Observations from HadISST1 (black solid), HadISST2 (black dotted) and the NOAA/NSIDC (blue) are shown, whereas the SPEAR_LO_DCIS is shown with a red line. Orange shades indicate one and minus one standard deviations of the SIE anomalies simulated from 30 ensemble members of SPEAR_LO_DCIS. Gray arrows correspond to a low sea ice period (late 1970s-1990s) and a high sea ice period (2000s-early 2010s). Correlation coefficient between HadISST1 and the SPEAR_LO_DCIS is shown in the bottom left where the asterisk indicates the statistically significant correlation at 90 % confidence level using Student's *t*-test. **(b-d)** Same as in **(a)**, but for the SIE anomalies in the Weddell Sea (60º-0ºW), Ross Sea (180º-120ºW), and Amundsen-Bellingshausen Sea (120º-60ºW), respectively.

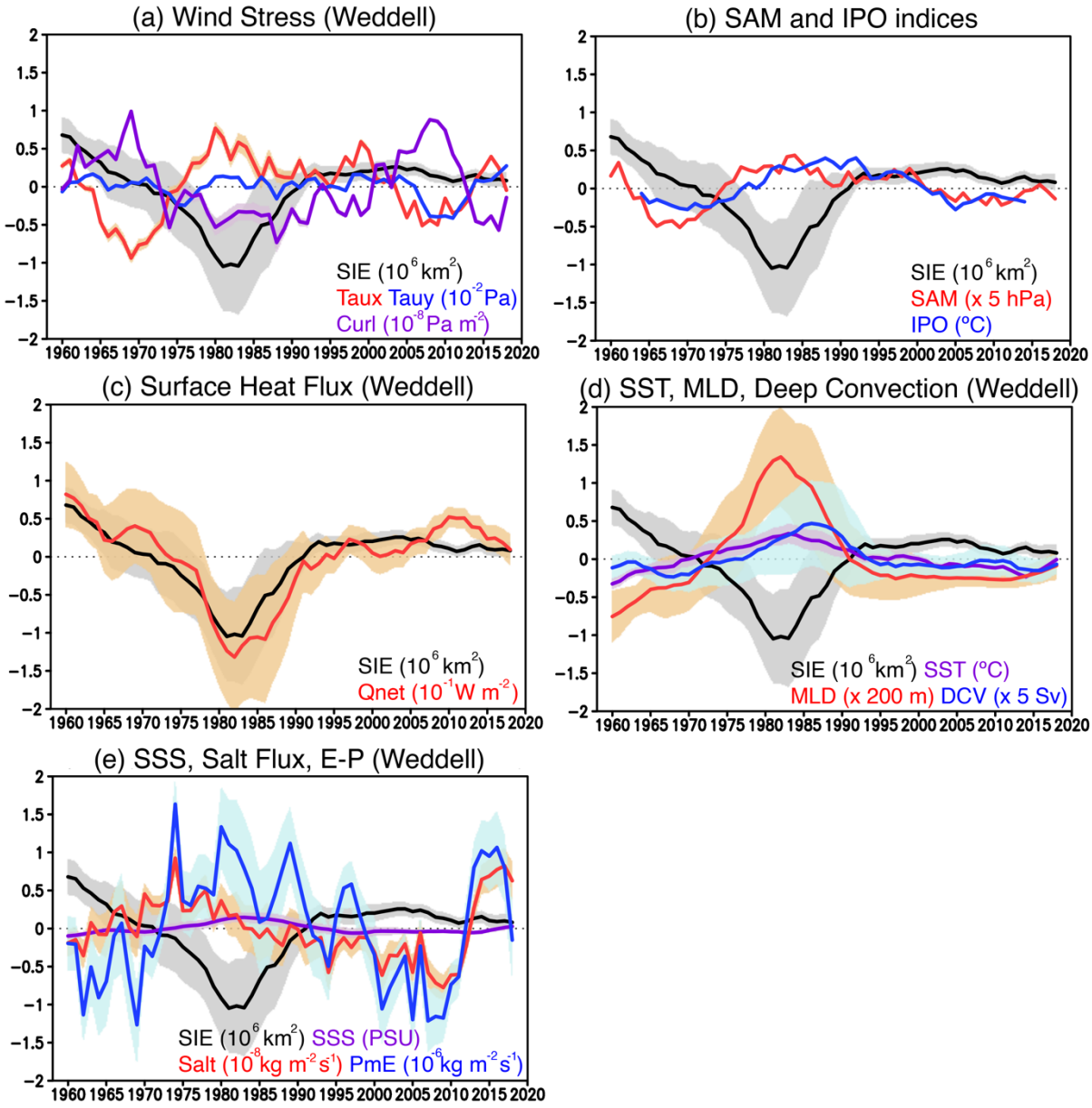

Figure 3 (a) Time series of 5-yr running mean SIE (black in 10^6 km^2), zonal (Taux; red in 10^{-2} Pa) and meridional (Tauy; blue in 10^{-2} Pa) wind stress, and wind stress curl (Curl; purple in 10^{-8} Pa m^{-2}) anomalies averaged in the Weddell Sea (60ºW-0º, south of 55ºS) during 1958-2020. Shades indicate one and minus one standard deviations of the anomalies from 30 ensemble members of the SPEAR_LO_DCIS. Positive wind stress curl anomalies correspond to downwelling anomalies in the ocean. **(b)** Same as in **(a)**, but for the 5-yr running mean SAM index (red in 5 hPa) and 13-yr running mean IPO index (blue in ºC). **(c)** Same as in **(a)**, but for the SIE (black in 10^6 km^2) and the net surface heat flux (Qnet; red in 10^{-1} W m^{-2}) anomalies. Positive surface heat flux anomalies correspond to more heat going into the ocean. **(d)** Same as in **(a)**, but for the SIE (black in 10^6 km^2), sea surface temperature (SST; purple in ºC), mixed-layer depth (MLD; red in 200 m), and deep convection (DCV; blue in 5 Sv) anomalies. **(e)**

Same as in **(a)**, but for the SIE (black in 10^6 km^2), sea surface salinity (SSS; purple in PSU), salt flux (Salt; red in 10^{-8} kg m^{-2} s^{-1}), and precipitation minus evaporation (PmE; blue in 10^{-6} kg m^{-2} s^{-1}) anomalies. Positive salt flux anomalies correspond to anomalous salt going into the ocean at the surface associated with sea ice formation, whereas the positive PmE anomalies mean more freshwater going into the ocean.

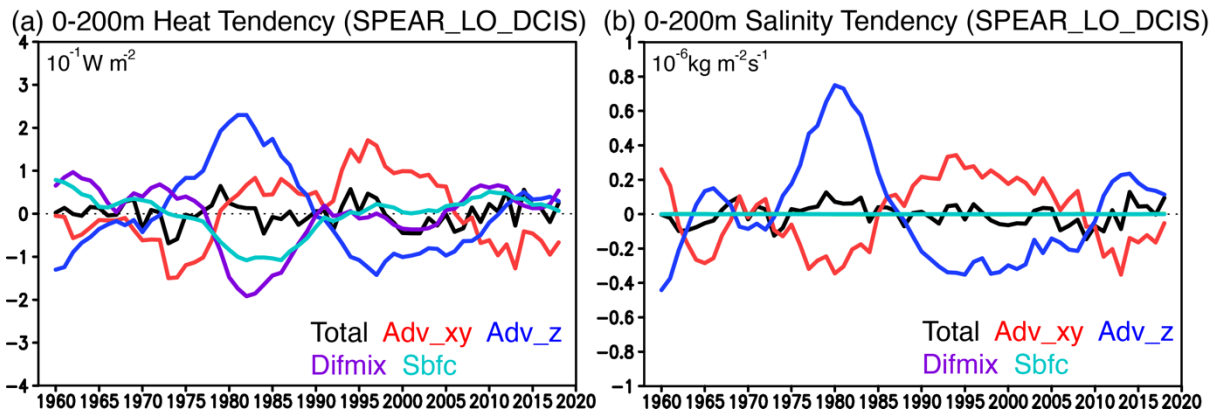

Figure 6 (a) Time series of 5-yr running mean ocean heat tendency (in 10^{-1} W m^{-2}) anomalies in the upper 200 m of the Weddell Sea from the SPEAR_LO_DCIS. Total ocean heat tendency (Total; black), horizontal advection (Adv_xy; red), vertical advection (Adv_z; blue), mesoscale diffusion and dianeutral mixing (Difmix; purple), and surface boundary forcing (Sbfc; light blue) anomalies are shown, respectively. **(b)** Same as in **(a)**, but for the salinity tendency (in 10^{-6} kg m^{-2} s^{-1}) anomalies.

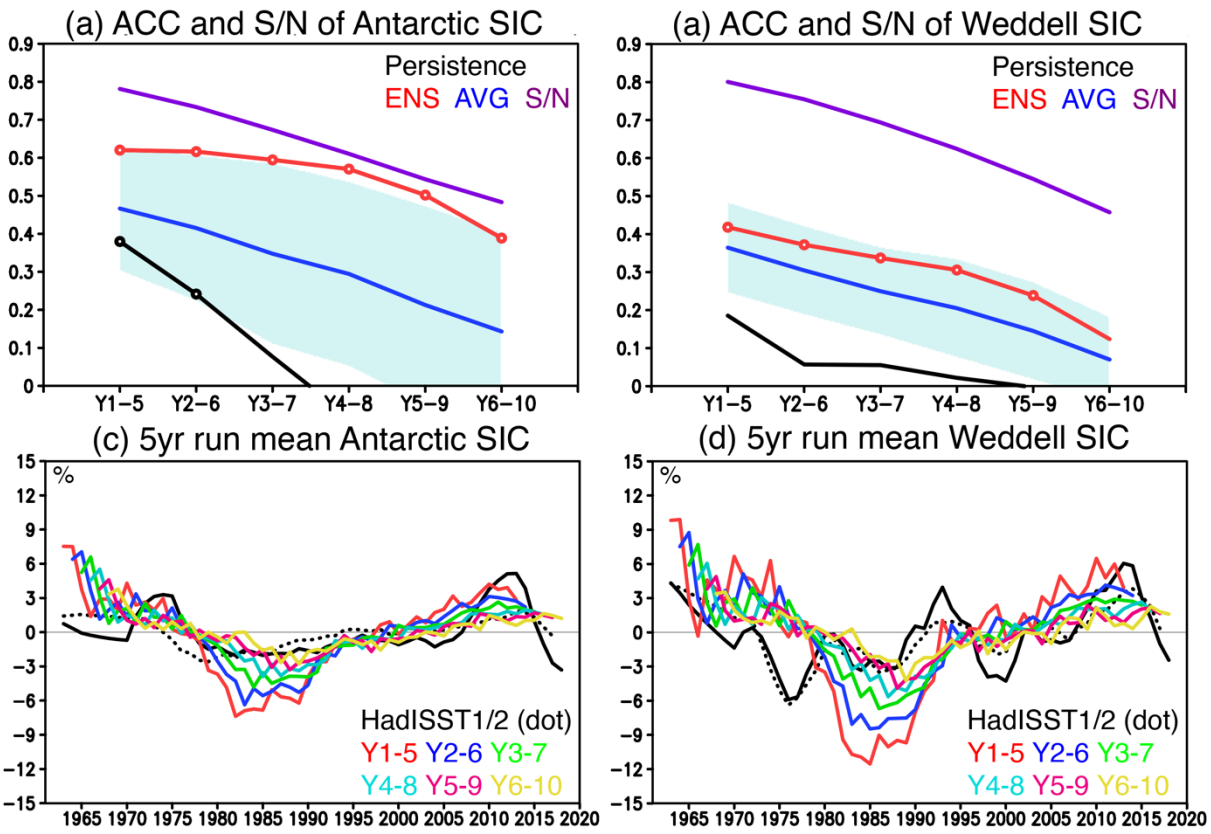

Figure 9 (a) ACC and signal-to-noise (S/N) ratio of pan-Antarctic (area-weighted mean) SIC anomalies predicted at lead times from 1-5 years to 6-10 years. The ACCs from the persistence prediction (black) and the SPEAR_LO_DRF ensemble mean (red), which are statistically significant at 90 % using Student's *t*-test, are described with open circles. The average of individual members' ACCs from the SPEAR_LO_DRF (blue) is shown with its one standard deviation (light blue shade). The S/N ratio from the SPEAR_LO_DRF (purple) is also plotted. **(b)** Same as in **(a)**, but for the ACC and S/N ratio of the SIC anomalies averaged in the Weddell Sea. **(c)** Time series of 5-yr running mean pan-Antarctic SIC (in %) anomalies during 1961-2020. Black lines show the observed SIC anomalies from HadISST1 (solid line) and HadISST2 (dotted line), whereas other colored lines correspond to the ensemble mean SIC anomalies predicted at lead times from 1-5 years to 6-10 years in the SPEAR_LO_DRF. **(d)** Same as in **(c)**, but for the SIC anomalies averaged in the Weddell Sea.

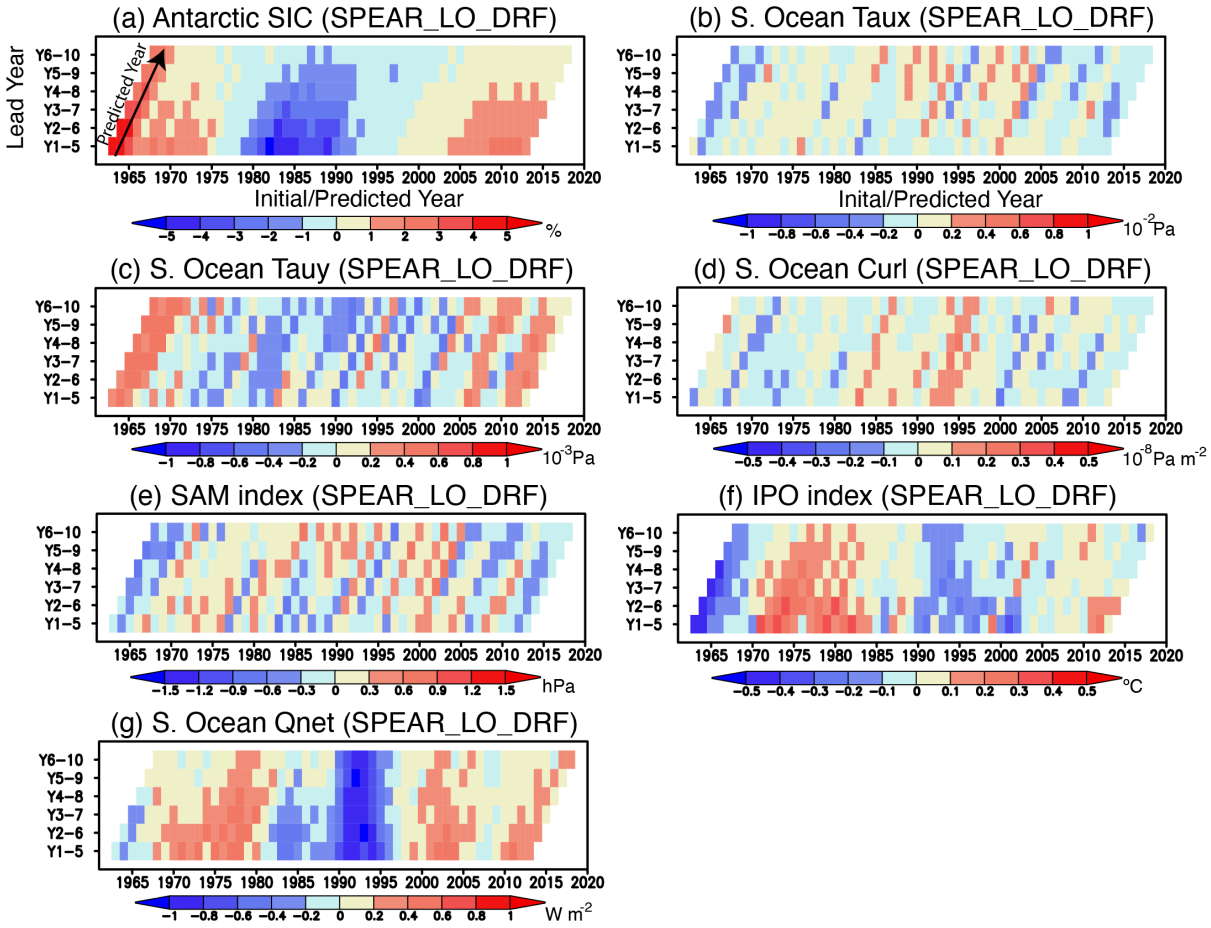

Figure 10 (a) Temporal evolution of ensemble mean pan-Antarctic SIC anomalies predicted at lead times from 1-5 years to 6-10 years in the SPEAR_LO_DRF as a function of initial/predicted years (x-axis) and lead years (y-axis). A black arrow indicates the correlations with the same initial year for different lead times, while the corresponding x-axis indicates the predicted years. **(b-d)** Same as in **(a)**, but for the zonal wind stress (Taux; 10^{-2} Pa), meridional wind stress (Tauy; 10^{-3} Pa), and wind stress curl (Curl; 10^{-8} Pa m^{-2}) anomalies averaged in the Southern Ocean (south of 55ºS). Positive wind stress curl anomalies correspond to downwelling anomalies in the ocean. **(e-f)** Same as in **(a)**, but for the SAM (in hPa) and IPO (in ºC) indices, respectively. **(g)** Same as in **(b)**, but for the net surface heat flux anomalies (in W m^{-2}). Positive surface heat flux anomalies indicate more heat going into the ocean.

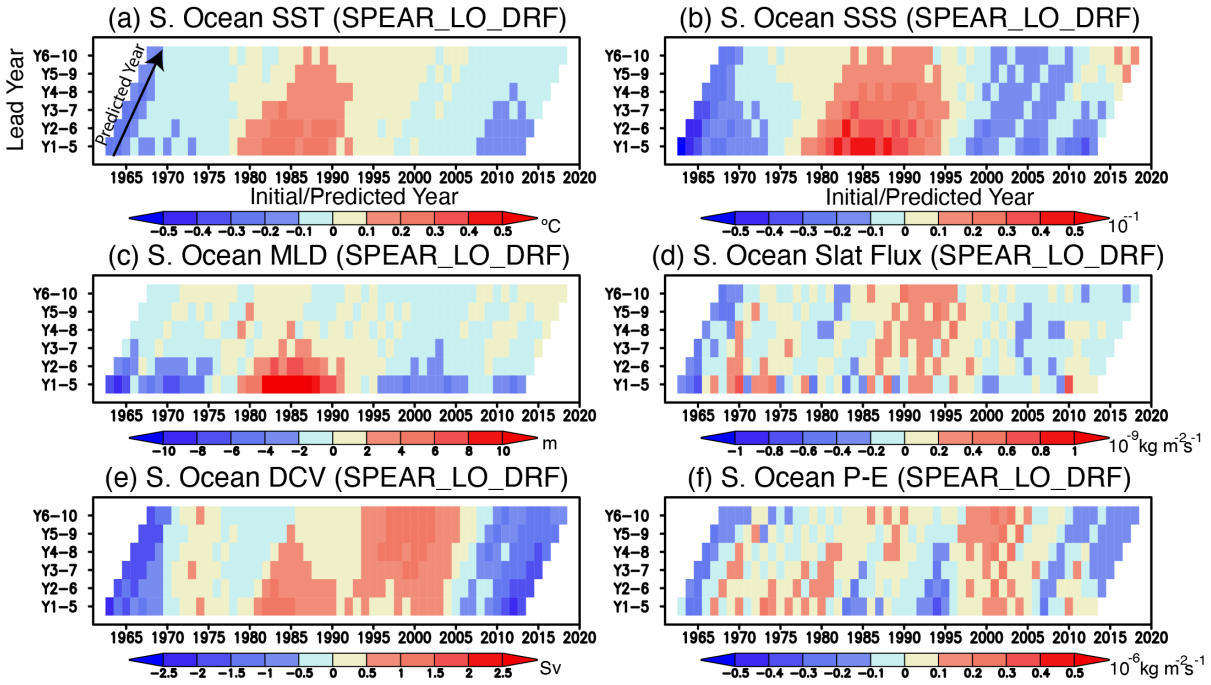

Figure 11 (a) Temporal evolution of ensemble mean Southern Ocean (south of 55ºS) SST anomalies predicted at lead times from 1-5 years to 6-10 years in the SPEAR_LO_DRF as a function of initial/predicted years (x-axis) and lead years (y-axis). A black arrow indicates the correlations with the same initial year for different lead times, while the corresponding x-axis indicates the predicted years. **(b-f)** Same as in **(a)**, but for the SSS (in 10^{-1} PSU), mixed-layer depth (MLD; in m), salt flux (in 10^{-9} kg m^{-2} s^{-1}), deep convection (DCV; in Sv), and precipitation minus evaporation (P-E; in 10^{-6} kg m^{-2} s^{-1}) anomalies averaged in the Southern Ocean, respectively.

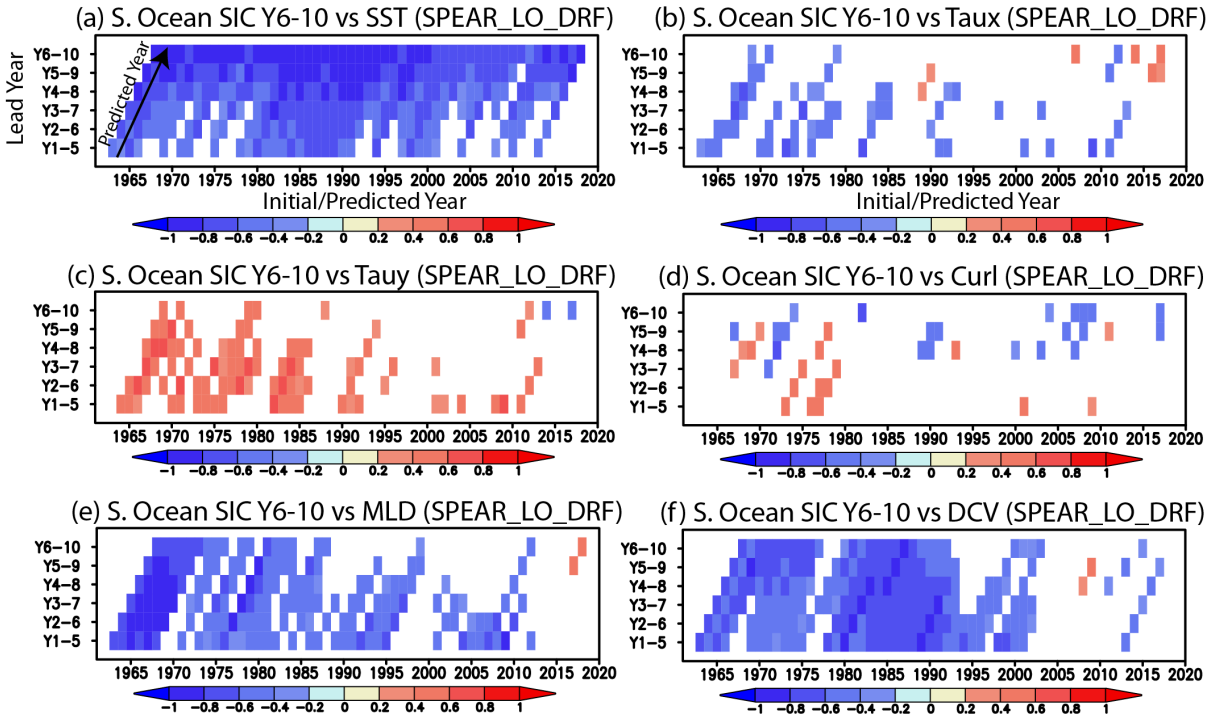

Figure 12 (a) Temporal evolution of inter-member correlation between the pan-Antarctic SIC anomalies predicted at a lead time of 6-10 years and the Southern Ocean SST anomalies predicted at lead times from 1-5 years to 6-10 years for the 20 ensemble members of the SPEAR_LO_DRF as a function of initial/predicted years (x-axis) and lead years (y-axis). A black arrow indicates the correlations with the same initial year for different lead times, while the corresponding x-axis indicates the predicted years. Correlation coefficients that are statistically significant at 90 % using Student's *t*-test are colored. **(b-f)** Same as in **(a)**, but for the inter-member correlation with the zonal wind stress, meridional wind stress, wind stress curl, mixed-layer depth, and deep convection anomalies averaged in the Southern Ocean.

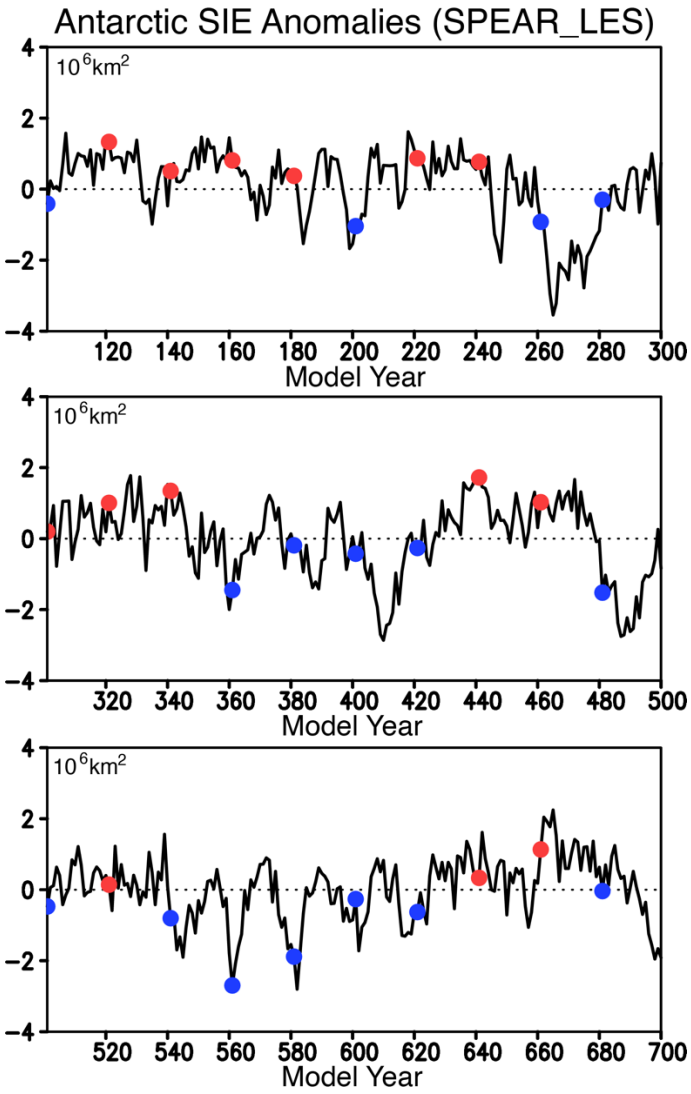

Figure S1 Time series of Antarctic SIE anomalies (in 10^6 km^2) from 101 to 700 years for the SPEAR_LES. Red and blue dots indicates the SPEAR_LO_DCIS start years (101, 121, …, 681 with 20 years interval) with positive and negative SIE anomalies to generate large ensemble members.

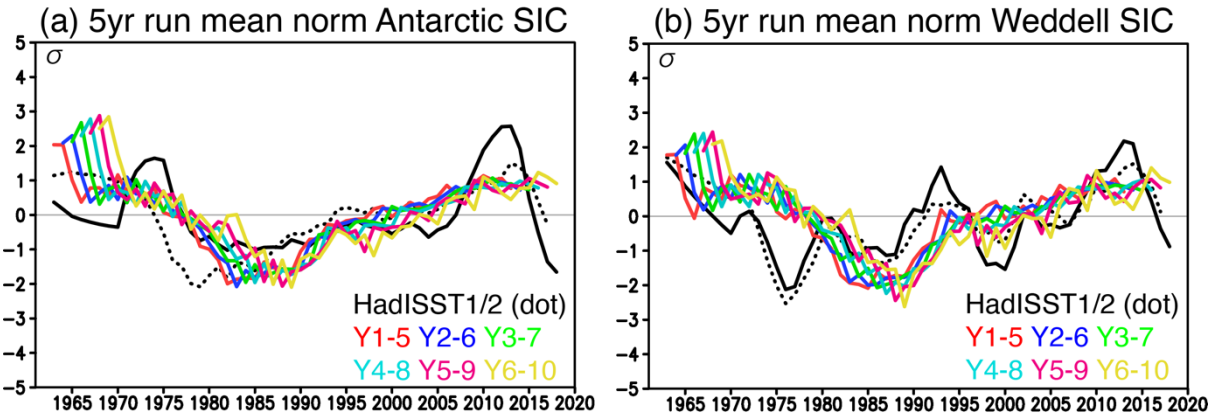

Figure S8 (a) Time series of 5-yr running mean pan-Antarctic SIC (in σ) anomalies normalized by standard deviation during 1961-2020. Black lines show the observed SIC anomalies from HadISST1 (solid) and HadISST2 (dotted), whereas other colored lines correspond to the ensemble mean normalized SIC anomalies predicted at lead times from 1-5 years to 6-10 years in the SPEAR_LO_DRF. **(b)** Same as in **(a)**, but for the normalized SIC anomalies averaged in the Weddell Sea.